Received: 14 March 2023 | Revised: 10 March 2024 | Accepted: 18 March 2024

DOI: 10.1111/all.16121

Allergy EUROPEAN JOURNAL OF ALLERGY AND CLINICAL IMMUNOLOGY EAACI WILEY

ORIGINAL ARTICLE

Atopic Dermatitis, Urticaria and Skin Disease

Mapping the immune cell landscape of severe atopic dermatitis by single-cell RNA-seq

Seon-Pil Jin[1,2,3] | Kyungchun Lee[4,5] | Yoon Ji Bang[6] | Yun-Hui Jeon[1,3] | Sunyoung Jung[6] | So-Jung Choi[6] | Ji Su Lee[1,3] | Junhan Kim[4,5] | Emma Guttman-Yassky[7] | Chung-Gyu Park[6,8,9] | Hyun Je Kim[6,8,9,10] | Seunghee Hong[4,5] | Dong Hun Lee[1,2,3]

[1]Department of Dermatology, Seoul National University Hospital, Seoul, Korea

[2]Department of Dermatology, Seoul National University College of Medicine, Seoul, Korea

[3]Institute of Human-Environmental Interface Biology, Medical Research Center, Seoul National University, Seoul, Korea

[4]Department of Biochemistry, College of Life Science and Biotechnology, Yonsei University, Seoul, Korea

[5]Brain Korea 21 (BK21) FOUR Program, Yonsei Education & Research Center for Biosystems, Yonsei University, Seoul, Korea

[6]Department of Biomedical Sciences, Seoul National University Graduate School, Seoul, Korea

[7]Department of Dermatology, Icahn School of Medicine at Mount Sinai, New York, USA

[8]Department of Microbiology and Immunology, Seoul National University College of Medicine, Seoul, Korea

[9]Seoul National University Hospital, Seoul, Korea

[10]Genomic Medicine Institute, Medical Research Center, Seoul National University, Seoul, Korea

Correspondence
Dong Hun Lee, Department of Dermatology, Seoul National University College of Medicine, 103 Daehak-ro, Jongno-gu, Seoul 03080, Korea.
Email: ivymed27@snu.ac.kr

Seunghee Hong, Department of Biochemistry, College of Life Science and Biotechnology, Yonsei University, 50, Yonsei-ro, Seodaemun-gu, Seoul 03722, Korea.
Email: seungheehong@yonsei.ac.kr

Hyun Je Kim, Department of Microbiology and Immunology, Seoul National University College of Medicine, 103 Daehak-ro, Jongno-gu, Seoul 03080, Korea.
Email: hjkim0518@gmail.com

Abstract

Background: Efforts to profile atopic dermatitis (AD) tissues have intensified, yet comprehensive analysis of systemic immune landscapes in severe AD remains crucial.

Methods: Employing single-cell RNA sequencing, we analyzed over 300,000 peripheral blood mononuclear cells from 12 severe AD patients (Eczema area and severity index (EASI) > 21) and six healthy controls.

Results: Results revealed significant immune cell shifts in AD patients, including increased Th2 cell abundance, reduced NK cell clusters with compromised cytotoxicity, and correlated Type 2 innate lymphoid cell proportions with disease severity. Moreover, unique monocyte clusters reflecting activated innate immunity emerged in very severe AD (EASI > 30). While overall dendritic cells (DCs) counts decreased, a distinct Th2-priming subset termed "Th2_DC" correlated strongly with disease severity, validated across skin tissue data, and flow cytometry with additional independent severe AD samples. Beyond the recognized role of Th2 adaptive immunity, our

Abbreviations: AD, atopic dermatitis; ASDC, *AXL*+SIGLEC6+dendritic cell; cDCs, conventional dendritic cells; DCs, dendritic cells; DE junction, dermis–epidermis junction; DEGs, differentially expressed genes; EASI, Eczema Area and Severity Index; EASI75, 75% reduction of clinical severity score EASI; HC, healthy control; IL, interleukin; ILCs, innate lymphoid cells; ILC2, group 2 innate lymphoid cell; IRF4, interferon regulatory factor 4; ISGs, interferon-stimulated genes; MO, monocyte; MigDC, migratory dendritic cell; mRegDCs, mature DCs enriched in immunoregulatory molecules; NK, natural killer; PBMCs, peripheral blood mononuclear cells; pDCs, plasmacytoid dendritic cells; SCGs, subcluster groups; scRNA-Seq, single-cell RNA sequencing; STAT6, signal transducer and activator of transcription 6; TF, transcription factor; TNFR, tumor necrosis factor receptor; UMAP, Uniform Manifold Approximation and Projection.

Seon-Pil Jin and Kyungchun Lee contributed equally to this article.

Funding information
National Research Foundation of Korea, Grant/Award Number: 2022M3A9D3016848, 2020R1F1A1073692, 2022R1F1A1075235 and 2022R1A2C10066566; Younsei University Research Fund, Grant/Award Number: 2022-22-0296

findings highlight significant innate immune cell alterations in severe AD, implicating their roles in disease pathogenesis and therapeutic potentials.

Conclusion: Apart from the widely recognized role of Th2 adaptive immunity in AD pathogenesis, alterations in innate immune cells and impaired cytotoxic cells have also been observed in severe AD. The impact of these alterations on disease pathogenesis and the effectiveness of potential therapeutic targets requires further investigation.

KEYWORDS
atopic dermatitis, chronic inflammatory disease, innate immunity, severe atopic dermatitis, single-cell RNA-Seq

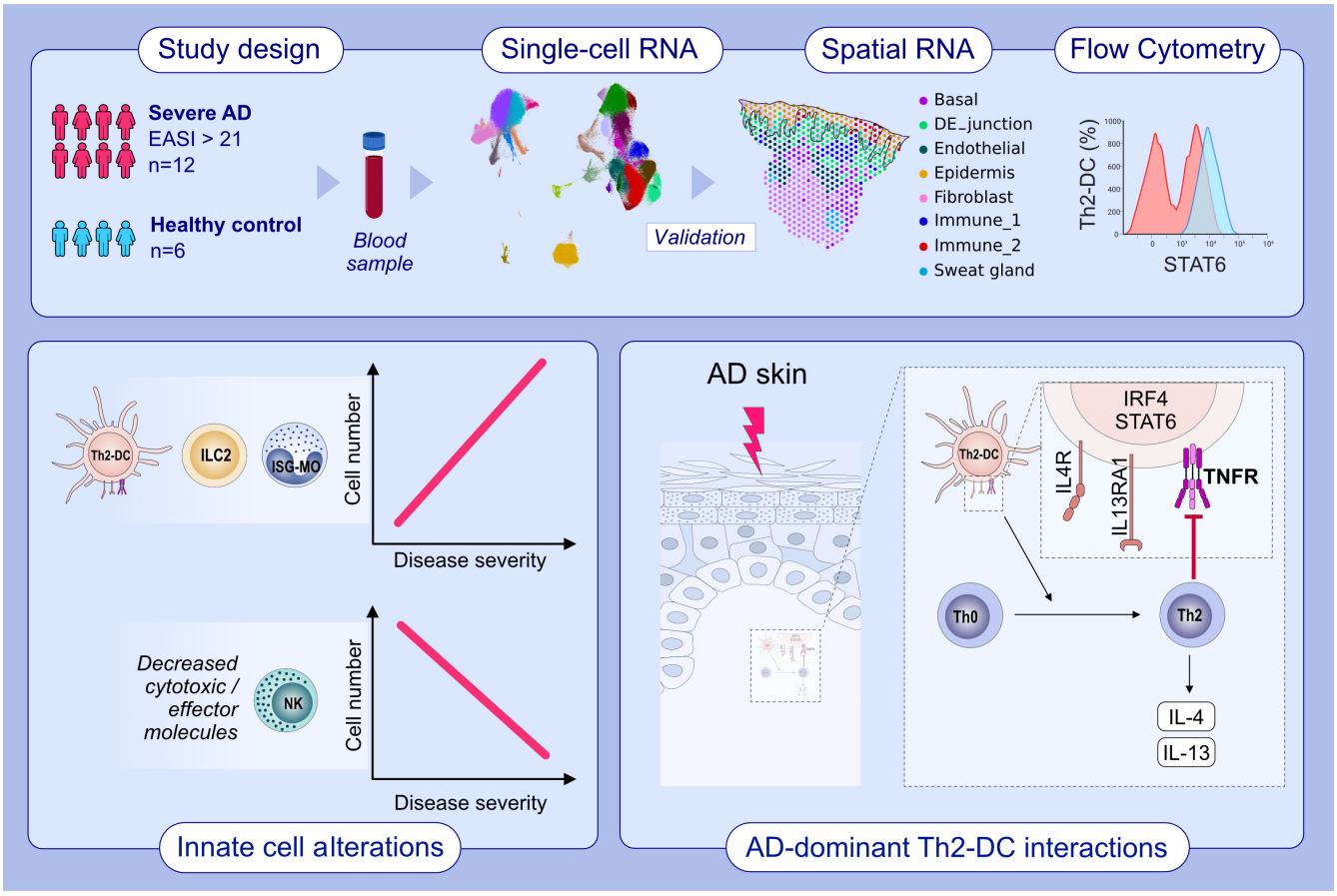

GRAPHICAL ABSTRACT

We analyzed blood samples from 12 patients with severe atopic dermatitis (EASI > 21) using single-cell RNA sequencing. Additionally, we validated our findings with skin single-cell spatial sequencing and flow cytometry. Our findings revealed a strong correlation between disease severity and the expansion of ILC2s and ISG-monocytes. Conversely, the number of natural killer (NK) cells was decreased in the patients, and the expression of cytotoxic/effector molecules in NK cells was negatively correlated with disease severity. Moreover, our study identified severe AD-dominant Th2-DCs that exhibited features of Th2-priming DC signals and interacted with Th2 cells residing in AD lesional skin.
Abbreviations: AD, atopic dermatitis; DC, dendritic cell; DE_junction, dermis epidermis junction; EASI, eczema area and severity index; IL, interleukin; ILC2, group 2 innate lymphoid cell; IRF4, interferon regulatory factor 4; ISG, interferon-stimulated genes; MO, monocyte; NK, natural killer cell; STAT6, signal transducer and activator of transcription 6; TNFR, tumor necrosis factor receptor.

1 | INTRODUCTION

Atopic dermatitis (AD) is a common chronic inflammatory skin condition, the prevalence of which varies between populations and affects 3%–10% of adults and ~20% of children.[1] A higher AD prevalence of 7%–10% has been reported in Asian adults AD.[2]

Atopic dermatitis is mediated via Th2-centered inflammation and exhibits significant heterogeneity on the basis of age, chronicity, ethnicity, and underlying endotypes.[2] The central mechanism involves Th2/Th22 cell immune response along with other immune cell dysregulations, including interactions between inflammatory dendritic cells (DC) and inflammatory stromal cells.[3–5] The Th1, Th22, and/or

Th17 pathways may be involved to varying degrees, and studies have demonstrated greater Th17 skewing in Asian patients from Korean and Japanese cohorts as compared to that in European American patients, thus highlighting the need for population-based studies.[4]

To date, AD immunology has been thought to activate acquired immunity, especially in T helper cells, through various antigens. However, recent studies suggest that innate immune cells, including basophils and innate lymphoid cells (ILCs), may be a possible source of Type 2 cytokines in AD lesions.[6] Additionally, alarmin class of cytokines, such as IL-1 and IL-18 produced by DCs and macrophages, are thought to induce Type 2 cytokine production in AD lesions without prior antigen exposure.[7] A subset of mature DC was identified as contributing to the maintenance of the immune environment in AD, even after clinical clearance following targeted treatment.[8] Consequently, the conventional understanding that AD pathogenesis is an acquired immune disease has thus been challenged, emphasizing the importance of an unbiased understanding of the immune cell landscape in AD patients.

Patients with moderate-to-severe AD have been reported to exhibit systemic immune abnormalities.[9] However, there is a scarcity of literature on severe (EASI > 21) AD patient's peripheral blood mononuclear cells (PBMCs) single-cell RNA sequencing (scRNA-Seq). Previous AD scRNA studies lacked consideration for the disease's severity (EASI), while our study is distinctly centered on a high-severity cohort.[5,8,10] Our study focuses on systemic dysregulation of innate immune cells from a narrow scope of AD patients, obtaining over 300,000 cells from mean EASI score of 27.8 AD patients and healthy controls (HC).

2 | MATERIALS AND METHODS

This study was approved by the Institutional Review Board at Seoul National University Hospital (IRB#H-1908-031-1052) and was conducted according to the Declaration of Helsinki; written informed consent was received from all subjects.

PBMC samples from 12 AD patients and six HC were collected and processed using the 10X version 1.1 Genomics 5′ Kit, Cellranger ver 6.1.2, followed by analysis by Scanpy ver 1.8.2. For preprocessing and quality control (QC), cells were filtered using a mitochondrial gene percentage threshold of under 15% and gene counts between 200 and 4000. All data were log-normalized. A total of 2000 highly variable genes were identified using pp.highly_variable_genes (flavor="seurat_v3"), and dimensionality was reduced using PCA component analysis (n_comps = 45). Doublets were further removed using the Scrublet package and manually curated by setting optimal transcriptome thresholds for each sample. Batch corrections were performed using the Harmony package (theta = 2.0, lambda = 10, sigma = 0.2, batch_key="sample"), projected using the UMAP method, and subsequently, clusters were defined by Leiden (resolution differed by cell type).

Each cell type cluster annotation and technical doublet were considered using canonical marker genes and DEG analysis. Overall, 301,068 cells were filtered into 277,808 cells post subcluster-level filtering. Gene Set Enrichment Analysis was performed using gProfiler and GSEApy enrichment methods with filtered DEGs. Further, transcription factor analysis was performed by the pySCENIC package ver 0.12.0, using GRNboost2 and arboreto, and gene scoring was carried out using the AUCell method on each cell type lineage. Trajectory analysis was performed using the PAGA method on Leiden-divided clusters, and the DPT function for the pseudotime analysis. Analysis of intercellular interaction that was conducted separately for disease groups was performed using the CellPhoneDB package ver 4.0.0 by degs_analysis, with input DEGs filtered by log2FC > 0.2, threshold = 0.1.

Detailed Methods and Materials have been uploaded as Data S1 to the repository.

3 | RESULTS

3.1 | Differentially expanded PBMC subsets in AD patients as revealed by scRNA-Seq

The transcriptomes of ~316,300 PBMCs from 12 severe AD and six HC samples were analyzed at single-cell resolution. Disease activity was measured for all 12 patients using the Eczema area and severity index (EASI) score (mean 27.8 ± 6.9), prior to categorization into severe (21 < EASI score < 30; $n = 8$) and very severe (30 ≤ EASI score; $n = 4$) groups. Patient demographics and clinical information are summarized in Tables S1 and S2, our schematics in Figure 1A. Unsupervised clustering by Uniform Manifold Approximation and Projection (UMAP), after correction for batch effect, revealed 27 molecularly distinct clusters (Figure 1B,C and Table S3).

Differentially populated cell clusters were observed in relation to disease status (AD vs. HC) (Figure 1D,E). The subsets that were increased in patients with AD included C8_CD4_Memory_T, C16_CD14_Monocyte, and C17_Proliferating T subsets. Those that were decreased in AD included DCs and NK cells, namely C2_NK, C20_pDC, C23_KLRC2_NK, and C26_cDC1. The remaining (20 out of 27) subsets were similarly represented, regardless of disease.

3.2 | CD4+ memory T cells and proliferating lymphocytes are expanded in AD

Further subclustering of T and NK cell subsets (174,317 cells) among PBMCs yielded 19 clusters (L0–L18; Figure 2A,B). AD is a Th2-driven disease,[11] and the UMAP of selected clusters confirmed an expansion of L6 (CD4+ memory T) and L13 (proliferative lymphocytes) clusters in AD in comparison to that of HC (Figure S1A). Upstream transcription factor (TF) prediction analysis using pySCENIC[12] identified GATA3- and FOXP3-regulating single-cell areas in the L2_CD4_Effector_T_1, L6_CD4_Memory_T, and L10_CD4_Effector_T_2 clusters (Figure S1B and Figure 2D). These cells were further validated by differentially expressed genes (DEGs) (Table S4) and the AUCell scoring system using known markers of Th2 and Treg cells (Table S5 and Figure S1C). Th2 and Treg levels were significantly increased in AD as previously reported.

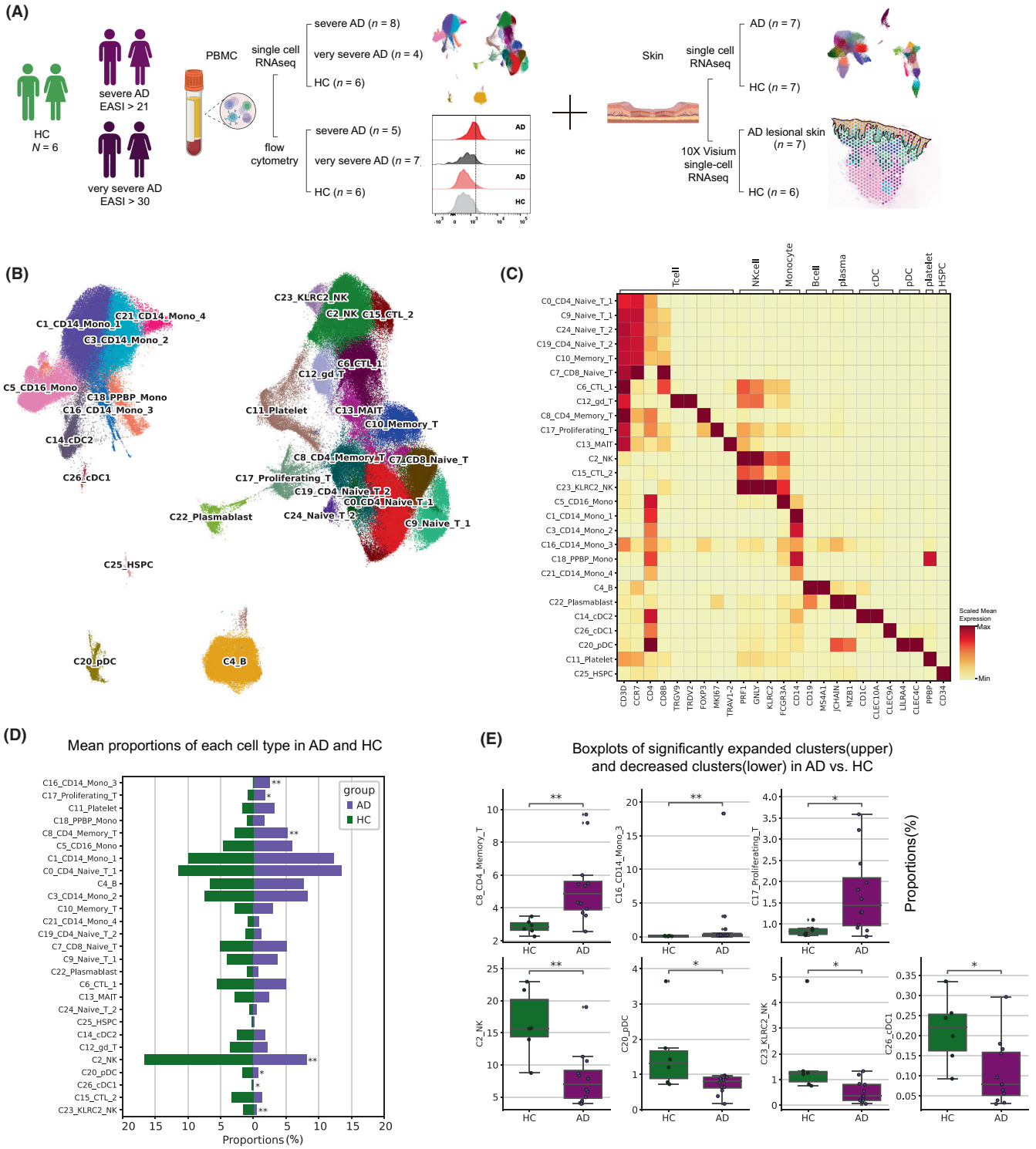

FIGURE 1 Single-cell RNA-Seq analysis highlights a distinct PBMC composition between AD and HC. (A) Schematics of AD PBMC analysis following validation with AD skin public data and additional patients PBMC flow cytometry (B) Uniform manifold approximation and projection (UMAP) plot showing PBMCs from merged data of 12 AD patients and six HCs, as 27 colored clusters. (C) Cluster annotations using selected marker genes. Color intensity indicates scaled mean expression level. (D) Bar plot representing mean proportions of each cell type in AD and HC group. *p* Values were calculated using the Kruskal–Wallis test (*, $p < .05$; **, $p < .01$). (E) Significantly increased (upper panel) or decreased (lower panel) clusters in AD as compared to that in HC. Each dot indicates individual subjects. *p* Values were calculated using the Kruskal–Wallis test (*, $p < .05$; **, $p < .01$; ***, $p < .001$; ****, $p < .0001$). The midline represents the mean value. Maximum length of the plot with whiskers as a proportion of the interquartile range. Whiskers extend to the furthest datapoint within the range. Outliers were defined as bigger or smaller than median $\pm 1.5 \times$ interquartile range.

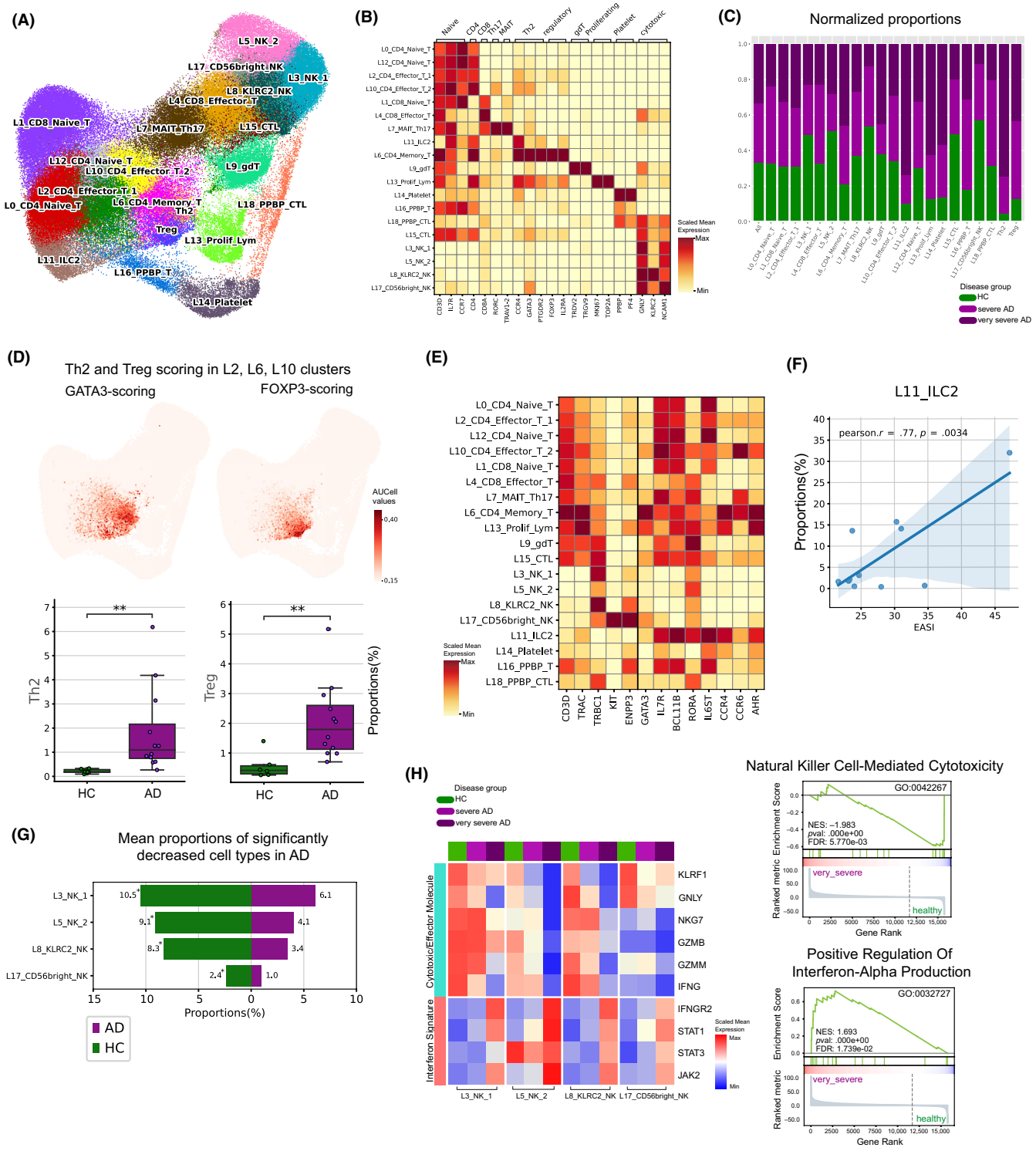

FIGURE 2 Subclustering analysis of T and NK cells showing functional dysregulation in AD. (A) UMAP plot displaying 19 subclusters of lymphoid cells. (B) Marker genes of each subcluster visualized by heatmap. (C) Relative proportions of disease groups in each subcluster. (D) Upper panel: transcription factor analysis performed using the regulatory network inference tool (pySCENIC) to identify GATA3 and FOXP3 regulatory regions in T cells. AUCell score was projected on UMAP plot for L2, L6, and L10 clusters to define Th2 (*GATA3+*) and Treg (*FOXP3+*). Lower panel: proportional boxplot for Th2 and Treg in overall T and NK cells. (E) Heatmap showing expression of negative and positive ILC2 marker genes. (F) Scatter plot between ILC2 proportions and EASI score. Linear fitting displayed as trendline, and light blue shadows indicate a 95% confidence interval. *p* Values were calculated by Student's *t*-test. *, $p < .05$; **, $p < .01$; ***, $p < .001$. (G) Averaged mean proportions of significantly increased cell subclusters among all NK cells in HC. *p* Values were calculated using the Kruskal–Wallis test (*, $p < 0.05$) (H) Left panel; Scaled gene expression level of indicated genes in NK cell subclusters (L3, L5, L8, and L17) from each disease group. Upper right panel; gseaplot of NK cells compared by very severe with healthy control showing decreased cytotoxicity. Lower right panel; gseaplot of NK cells compared by very severe group with healthy control showing elevated inter feron production. CTL, cytotoxic lymphoid cells; GO, Gene Ontology; Prolif_Lym, proliferative lymphoid cells.

3.3 | ILC2 correlated positively with disease severity in AD

In AD, the link between disease severity and the abundance of innate lymphoid cells type 2 (ILC2s) has been revealed, but the low frequency of ILCs within PBMCs, typically ranging from 0.1% to 1% in healthy individuals, complicates their detection using scRNA-Seq.[13,14] In line with this, the cluster we identified as ILC2s was found primarily in AD patients (87.4%), and was substantiated by distinct gene expression patterns indicative of ILC2, notably featuring positive expression of *IL7R*, *BCL11B*, and *RORA*, along with the absence of *CD3D*, *TRAC*, *TRBC1*, *KIT*, and *ENPP3* (Figure 2E).[15,16] Additionally, TF analysis identified *GATA3* as a prominent regulon in the ILC2 cluster (Figure S1D,E).[14] Moreover, the prominent upregulation of skin-homing chemokine receptors, specifically *CCR4* and *CCR6*, within this cluster, implies a potential migration from the cutaneous skin. Notably, the proportion of ILC2 exhibited a strong positive correlation with disease severity, as measured by EASI score ($r = .77$, $^{**}p < .01$) (Figure 2F). These findings underscore the potential role of ILC2s in the pathogenesis and progression of AD.

3.4 | AD demonstrated a decline in all types of NK cell clusters, each displaying defective cytotoxicity programs

Two subsets of NK cells were discerned based on CD56 expression: CD56 (*NCAM1*)-high and -low populations. Within CD56-low population, three subpopulations were identified, including (1) a cluster with high-expression levels of granzymes and *IFNG*, akin to the characteristics of the CD56dim population (referred to as L3_NK_1); (2) a cluster exhibiting diminished cytotoxic properties (L5_NK_2); and (3) memory-like or adaptive NK cells recognized by *KLRC2* expression, also known as *NKG2C* (L8_KLRC2_NK). Notably, in AD patients, there was a significant reduction in all NK cell clusters (L3, L5, L8, and L17) compared to that in the HCs (Figure 2G). Moreover, all NK cells in AD exhibited reduced expression of cytotoxicity (*GNLY*, *NKG7*, *KLRF1*, *GZMB*, *GZMM*, and *IFNG*), with a more pronounced decrease observed in the very severe group. Additionally, upregulation of the JAK–STAT pathways (*STAT3*, *JAK2*, *STAT1*, and *IFNGR2*) (Figure 2H) and increased expression of interferon-stimulated genes (ISGs) were observed in AD NK cells (Figure S1F).

3.5 | IgE-secreting B cells were expanded in AD and displayed IL4/13 signals

Upon analysis of B cells, eight distinct clusters (B0–B7; Figure S2A,B and Table S6) were identified. Cluster B5_IgE_B was exclusively found in very severe AD, and expressed the highest level of *IGHE* among all B-cell subsets (as illustrated in Figure S2C,D). Moreover, plasmablasts in AD also displayed elevated *IGHE* expression in comparison to those in HCs. (Figure S2E). Notably, the subsets B5 and B6, characterized by double-negative features (*IGHD*− *CD27*−), displayed significant upregulation of Type 2 signals (*IL13RA1*, *IL4R*, *STAT6*, and *JAK2*) in AD as compared to that in the HCs (Figure S2F).

3.6 | Monocytes with elevated interferon responses and TLR pathways were primarily found in very severe AD

Subclustering of the myeloid cells (80,187 cells) yielded 14 clusters (M0–M13) (Figure 3A,B and Table S7). Among these clusters, the proportions of three distinct monocyte subclusters (M1, M9, and M12) were exclusively expanded in the very severe AD group (Figure 3C–E). This expansion was accompanied with an upregulation of the Type I interferon and TLR/JAK–STAT pathways (Figure 3F,G), indicating activated innate immunity. The proportion of ISG-expressing monocytes showed a robust positive correlation with disease severity ($^{*}p < .05$, $r > .6$) (Figure S3A,B). Additionally, pDCs (M11_pDC), which were decreased overall in AD, were further subdivided into four subclusters (Figure 3G). Among these, ASDC (*AXL* + *SIGLEC6* + dendritic cell) subset exhibited inflammatory signatures (*IL1B*, *IL6R*, and *TNF*) distinct from other pDC subsets, yet this population did not show a significant association with AD (Figure 3H,I).

3.7 | A novel AD-dominant DC subset was discovered, particularly prevalent in very severe AD, which displayed activated Type 2 inflammation signature

Upon further subclustering, cDCs (M6_cDC) yielded seven subclusters (Figure 4A,B and Table S8). Among these, a distinct DC subset, exclusively expanded in very severe AD patients, exhibited similar characteristics (e.g., TLR signaling) with cDC3. However, it presented distinct transcriptome profiles and was named "Th2_DC" (Figure 4B–D). Unlike cDC3, which is characterized by upregulated ISGs, TNF, and chemokines, Th2_DC predominantly expresses the Notch signaling pathway (Figure 4D and Figure S4A,C).[17] The abundance of Th2_DC strongly correlated with disease severity ($r = .72$) (Figure 4E). Additionally, Th2_DC showed relatively low levels of migratory or maturation markers (e.g., *CCR7*, HLA-II, *CD86*, and *CD80*) as compared to those in mReg_DC and cDC3 (Figure S4B).

Th2_DC displayed signatures associated with skin-homing factors (*ITGA4*, *ITGB1*, and *CCR2*), with low-CD103 (*ITGAE*) and high-CD11c (*ITGAX*) levels. Notably, relatively lower expression of CD11b (*ITGAM*) was observed in Th2_DC compared to cDC3 (Figure 4D). Additionally, Th2_DC harbored prominent downstream signals of IL13 (*IL13RA1*, *IL4R*, and *STAT6*) with upregulated JAK–STAT pathways (Figure S4C,D), which is consistent with the previously reported features of Th2-promoting DCs.[18]

Conducting trajectory analysis on DC subsets revealed Th2_DC as the terminal point when initiated from CD1c_cDC (Figure 4F).

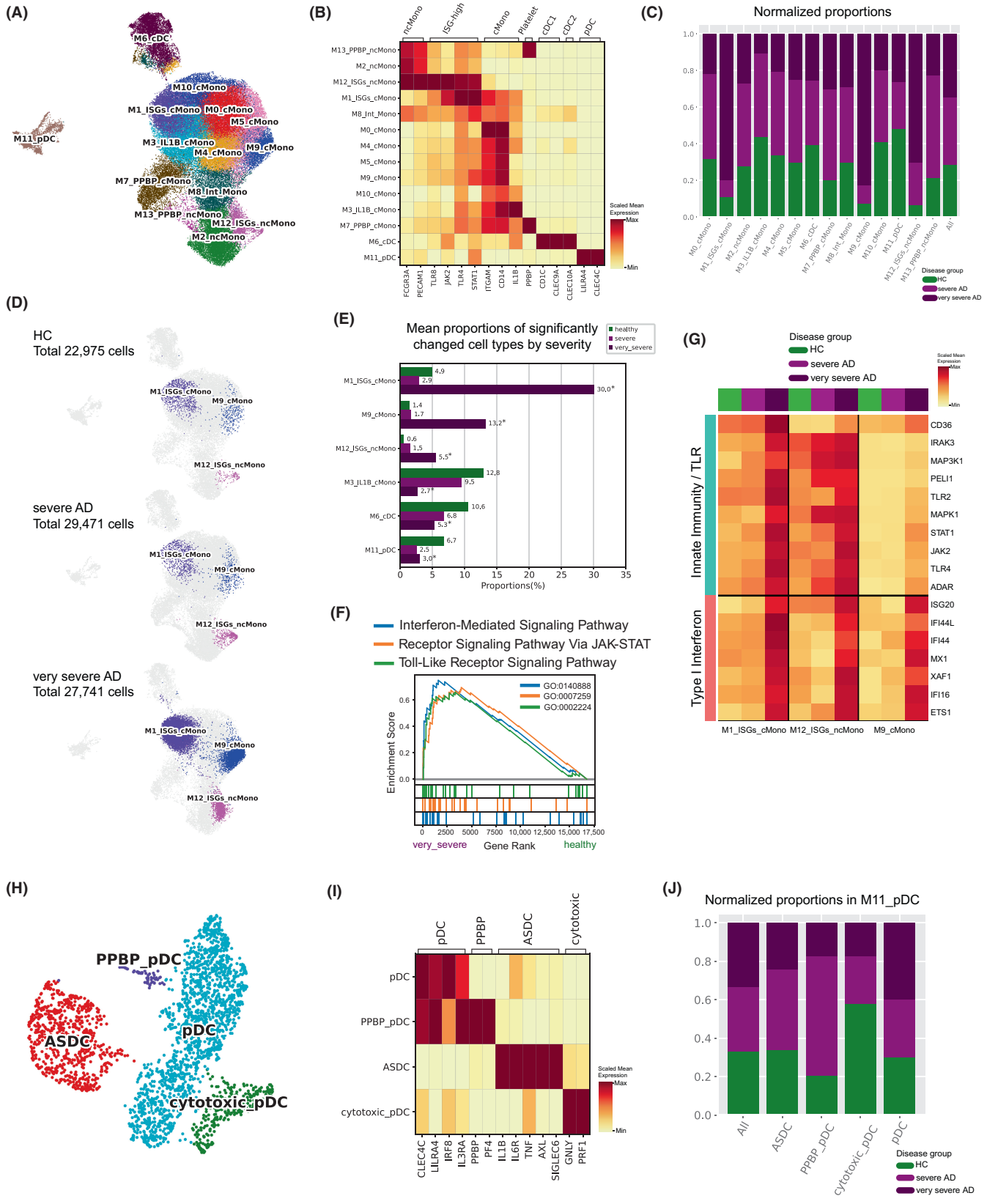

This pattern was conserved even when starting from cDC2 or cDC3 (Figure S4E). The TFs that governed the gene expression profiles of Th2_DC, as revealed by pySCENIC analysis, included unique regulons of *IRF4*, *NFKB1*, *NFATC1*, and *STATs*. Additionally, upregulation of *TLR2/4*, known components essential for stimulating and maintaining Th2 cells by DCs, were observed (Figure 4D,G,H).[19,20]

To identify molecules involved in Th2 cell interaction, a cell–cell interaction analysis between Th2_DC and Th2 cells using CellphoneDB was conducted (Figure 4I). By excluding overlapping interactions with the HC group or CD4 naive T cells (L0, L2, and L12) (Figure S5A,B), several AD-enriched receptor–ligand interactions between Th2_DC and Th2 cells were identified (Figure S5C). Notable

FIGURE 3 Monocytes with interferon signatures were predominant in very severe AD, showing activated innate immunity pathways. (A) UMAP plot of myeloid cell subclusters. (B) Selected representative marker expression in myeloid cells. (C) Relative proportions of disease groups in each subcluster. (D) Significantly expanded monocyte clusters (M1, 9, and 12) in very severe AD depicted on UMAP plot, and total myeloid cell number was shown on the plot in each disease group. (E) Mean proportions bar plot of significantly increased cluster in the disease group or HC. *p* values were calculated using the Kruskal–Wallis test (*, $p < .05$) (F) Gseaplot of M1, M9, and M12 clusters compared by very severe with healthy group showing elevated interferon, JAK–STAT, TLR pathways. (NES interferon: 1.99, JAK–STAT: 1.80, TLR: 1.75) NES: normalized enrichment score. TLR: toll-like receptor (G) Selected genes involving "innate immunity/TLR pathway" and "Type I interferon signature" as shown in the clusters (M1, 9, and 12) were increased in very severe AD. (H) UMAP Subclusters of pDCs. ASDC, AXL + SIGLEC6 + DC; pDC, plasmacytoid DC. (I) Expression of selected marker genes for pDC subclusters. (J) Relative proportions of disease groups in each subcluster of pDC.

interactions included the TNF family receptors (*TNFRSF1A/B* with *GRN*, *TNFRSF21* with *APP*) and *SIRPA* (with *CD47*), indicating inhibition of Th2_DC.[21–24] On the other hand, Th2 cells also expressed ligands that activate Th2_DC (*CD2*, *CD40LG*, *ICAM2*, and *ICAM3*). Th2_DC demonstrated *CD47* (to *SIRPG*), *TNFSF13* (to *TNFRSF14*), and *ICAM3* (to *LFA1*) expression, suggesting Th2-cell stimulation.[25,26] Moreover, Th2_DC and Th2 cells may interact via certain adhesive molecules (*SELPLG*, *SELL*, *ADGRE5*, and *CD55*) and prostaglandin signaling (*PTGER4*) (see also Figure S4D).[27–30]

3.8 | Cross validation of Th2_DC with spatial transcriptome of AD skin tissues and flow cytometry

To validate our observations regarding immune cell dynamics in PBMC and their representation in lesional skin, we cross-referenced our PBMCs findings with scRNA-Seq data obtained from AD skin provided by Liu et al.[10] Analyzing skin tissue cells (65,958 cells) and focusing on subclustered myeloid cell lineage specifically (15,845 cells), 12 clusters were identified (Figure 5A). By utilizing VISION score calculations[31] to compare the gene signatures extracted from Th2_DC in PBMCs with skin DCs, significant similarities were found in the expression profile. Notably, high expression levels in migDC_1 demonstrated a close resemblance to Th2_DC found in peripheral blood (Figure 5B). The significantly increased prevalence of migDC_1 in AD, along with the expression of chemokines and cytokines (*CCL17*, *CCL22*, and *IL15*), aligns with previously documented literature[5,8,32] identifying an inflammatory dendritic cell subset, thereby implicating the pathogenic role of migDC_1 (Figure S6B,C). A strong correlation between Th2-cell proportions and migDC_1 proportion ($r = .86$, $p < .0001$) indicates potential interplays between these cellular populations (Figure 5C). Furthermore, while skin NK cell frequencies were comparable between AD versus HC (Figure S6C), the downregulation of cytotoxic genes observed in PBMCs was corroborated in skin NK cells in AD patients (Figure 5D).

We analyzed spatial transcriptomics data from Mitamura et al.,[32] which encompassed both lesional and nonlesional skin samples of AD. In lesional skin, Immune_1 and Immune_2 clusters were primarily composed of mixed lymphoid and myeloid cells, respectively (Figure S6D). Employing Th2_DC gene sets (Figure 5B,E and Table S5), these clusters notably exhibited elevated expression of Th2_DC scores. Notably, the Immune_1 cluster displayed high Th2 geneset scores, suggesting a potential interaction between Th2_DC and lymphoid cells (Figure 5E and Figure S6D) in AD skin. In contrast, nonlesional skin predominantly showed low Th2_DC scores.

For further experimental validation, we performed flow cytometric analysis to validate Th2_DC from additionally collected PBMCs of individuals with AD ($N = 8$), HC ($N = 12$), and incorporated 4 AD samples (AD 3, 4, 5, and 6) that overlapped with those in our PBMC scRNA-Seq study (Figure S7A and Table S9). As previously shown in this study, the IL13 signal emerged as a key discriminator for Th2_DC among other DCs. To validate this, we stimulated DCs with rhIL-13 to assess the presence of IL13RA1 in Th2_DC. Notably, the proportions of phospho-STAT6 (pSTAT6)-positive cells within the total cDC population exhibited a significant increase; also within cDC2 and cDC3 population (Figure 5F and Figure S7B), indicating the presence of IL13RA1-positive cDCs.

Further analysis revealed a significant upregulation of Notch2 and CD206 (MRC1) in IL13RA1+ DCs (pSTAT6(+) cells) compared to pSTAT6(−) DCs in total cDC (Figure 5G and Figure S7C). This finding aligns with the exclusive expression of NOTCH2 and MRC1 in Th2_DC compared to other DCs in the transcriptome data (Figure 4B, see also Figure S6F). This observation supports the expansion of IL13RA1+ cDCs expressing elevated levels of Notch2 and CD206, indicating the presence of Th2_DC in AD PBMCs.

3.9 | Patient stratification by hierarchical clustering and differential gene signatures between subcluster groups

To explore the molecular stratification potential of PBMC scRNA-Seq, hierarchical clustering was performed to stratify patients based on their cell subcluster proportions. Strikingly, this resulted in the classification of patients into three branches that mostly corresponded with the three disease categories of patients. Patients of AD 4, 5, and 6 were segregated from those with severe AD, and represented the most severe cohort (EASI > 30). Five main subcluster groups (SCG1-5, Figure 6A) were identified, each displaying a distinct predominance pattern. While SCG3 was predominantly found in the HCs, SCG1 and SCG4 were upregulated in all AD patients, with SCG5 expanded specifically in the most severe cases (AD 4, 5, and 6). SCG1 primarily comprised naive cells showing central circulating features (*CCR7* and *SELL*), distinguishing it from SCGs 2, 4, and 5, which were increased in AD. SCG2 primarily consisted of myeloid cells, which exhibited a reduction in very severe AD as compared

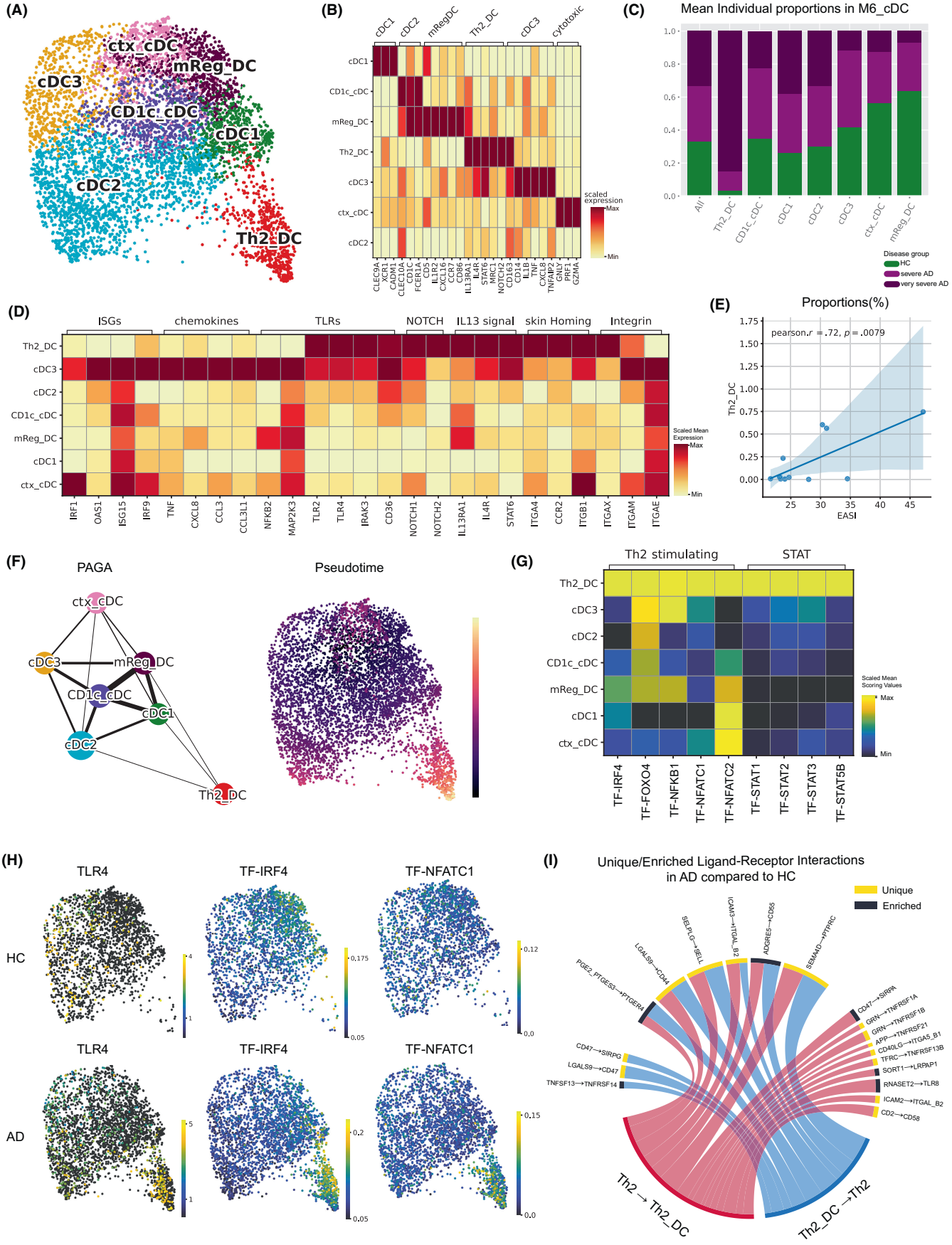

FIGURE 4 cDC subclustering analysis revealed potential Th2-priming DCs in very severe AD. (A) UMAP plot transferred from PAGA (partition-based graph abstraction)-initialized single-cell embeddings. cDC subclusters as separated from the cluster of M6_cDC in Figure 3A. (B) Expression of selected representative markers of cDCs. (C) Relative proportions of disease groups in each subcluster of cDC. (D) Expression of selected representative functional markers for Th2_DC subset. (E) Scatter plot for Th2_DC proportions and EASI score. Linear fitting displayed as trendline, and light blue shadows indicate a 95% confidence interval. (F) Left panel: PAGA-graph consisting of cell groups as nodes and weighted edges that represent a statistical measure of connectivity. Right panel: pseudotime calculated using "diffusion pseudotime" with CD1c_cDC as root cells. (G) Transcription factor analysis using regulatory network inference tool (pySCENIC) to identify regulators for the Th2_DC subset. AUCell score scaled and visualized on a heatmap. (H) Key transcription factors and the gene that specifically represented the Th2_DC subset. (I) Circos plot of potential ligand–receptor interactions from CellphoneDB between Th2 and Th2_DC. Comparison of mean expression level of ligand/receptor pair between AD and HC. Only interactions with higher expression levels in AD than that in HC are depicted.

to severe AD, while also presenting features of S100A molecules[11] and CSF3R pathway genes (*TYK2*, *STAT3*, and *SOCS3*), related to myeloid cell survival and proliferation.[33] SCG3 was representative of cytotoxic cells including NK cells and effector T cells, exhibiting a decrease in AD compared to HCs (Figure S8A). SCG4 encompassed CD4 memory T cells, Th2 cells, Tregs, and plasmablasts, demonstrating signatures linked to type I IFN responses (*IFNAR1/2*, *OAS1/2*, and *IRF9*), as well as associations with Th2/Th22-associated genes (*GATA3*, *CCR4*, *CCR6*, and *CCR10*), pivotal in AD pathogenesis. SCG5 was exclusively associated with very severe AD, displayed upregulation of IL13 signals, ISGs, TSLP, TLR, and Notch pathways (Figure 6B and Figure S8B).

4 | DISCUSSION

Atopic dermatitis, traditionally understood as a skin-centric condition, is now recognized as a systemic immune disorder characterized by Type 2 inflammation. Prior to the era of immune-targeted treatment (IL-4Rα, IL-13, and JAK), studies on AD were mostly focused on barrier dysfunction and skin inflammation in skin lesions.[34,35] However, recognizing AD as a systemic disease that affects the entire body, we aimed to elucidate the alteration of the systemic immune system in AD using single-cell RNA-Seq technology. We focused on severe AD cases (mean EASI = 27.8), as recent observations suggest that mild AD shows limited systemic features that are detectable in the bloodstream.[36]

Among the various immune subset changes in AD, a significant surge in Th2 cells, a hallmark feature of the disease, was evident in our findings (Figure 2D). Employing transcription factor prediction analysis and a gene set scoring, CD4+ memory T cells were found to have increased levels of Th2 and Treg cells (Figure S1B). Corresponding to previous studies reporting a reduction of NK-cell count in AD blood[37–39] we observed a striking impairment in the production of cytotoxic molecules and effector cytokines in all NK-cell subsets. The downregulation of *KLRF1* in severe AD, which encodes NKp80, an important receptor stimulating cytotoxicity and activating cytokine release including *IFNG* in mature NK cells, further emphasized this impairment.[40] Moreover, in line with these findings, the skin of individuals with AD showed parallel dysregulation of cytotoxic genes, confirming a consistent perturbation across PBMC and skin NK cells (Figure 5C). Previous research has suggested that reduced NK cell count in AD blood may be due to "activation-induced cell death" by cytokines in AD.[38] Our study uncovered the upregulation of apoptosis-related pathways in whole NK cells (L3, 5, 8, 17) in AD contexts compared to HC (Figure S1G). NK cells have been shown to regulate ILC2 in homeostasis,[38] and their deficiency has been observed to cause elevation of ILC2 in lesional tissue as well as systemic circulation in an AD-like mouse model.[38] Consistent with these reports, the ILC2 population was found to be elevated in very severe AD (Figure S1A) with a significant reduction in NK cells. Strong correlations were shown between EASI scores and ILC2 frequencies (Figure 2F). However, we did not focus on their direct contribution to AD pathology, leaving an intriguing avenue for future exploration. While ILC2s correlate with disease severity, targeting them alone might not be the key therapy, as shown by the lack of response to upstream cytokine neutralization (e.g., TSLP, IL-1α, and IL-33) in moderate-to-severe cases.[41–43] However, given the limitations of current medications, ILC2s could offer an additive benefit and likely play a role in pathogenesis. This underscores the complexity of AD and the need for multifaceted approaches targeting different immune aspects.

The three monocyte subsets (M1, M12, and M9) that were notably expanded in individuals with very severe AD (Figure 3D,E) showed upregulation of the TLR/JAK–STAT pathway and interferon signatures, indicating activation of innate immunity (Figure 3F,G and Figure S3A). The frequencies of these ISGs-high monocytes correlated with EASI scores (Figure S3B, $r > .6$), which may be indicative of severe inflammation in AD.

While the differentiation of CD4+ T cells into Th2 cells in the presence of IL-4 is well known, the mechanism that initiates Th2 differentiation is not well understood. Growing evidence suggests that certain DC populations, functioning as antigen-presenting cells, prime naive CD4+ T cells, thereby initiating the differentiation into Th2 cells.[44] These specialized DCs, known as DC^{Th2}, have been found to regulate Th2 polarization in skin and lung through the expression of IRF4.[45,46] The induction of *IRF4* occurs via *NFkB* and *NFAT* in lymphocytes and through TLR4 signaling in innate cells.[47,48] Additionally, Th2-inducing cytokines, such as *TSLP*, stimulate *IRF4* expression via *STAT5* in human DCs, further inducing the development of Th2 response.[49,50]

Recent studies underline the necessity of IL-13 for skin homeostasis in DCs promoting Th2 responses. These skin DC^{Th2} rely on *IL13*-mediated *STAT6* signaling pathway for their function. In addition to *IRF4* and *STAT6*, skin DC^{Th2} expresses other transcription factors like *FOXO4* and *NFATc1*, which are unique to this cell type in lung, skin, and small intestinal DCs. Compared

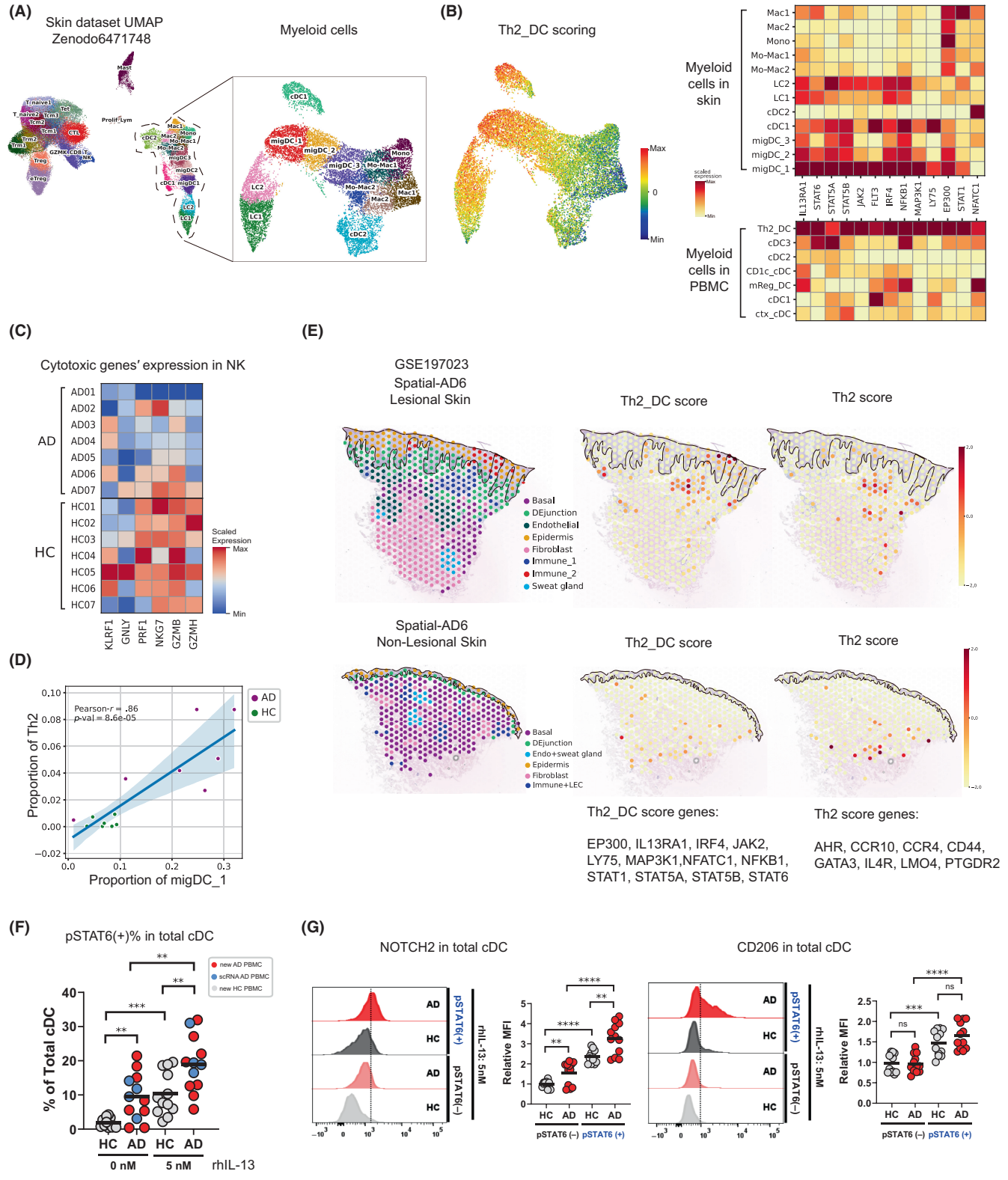

FIGURE 5 Validations of AD PBMC findings in skin AD and spatial-resolved data, flow cytometry gating (A) whole-skin cells UMAP; left panel. Skin myeloid cells UMAP; right panel (B) VISION scoring UMAP projection of Th2_DC genes on skin myeloid cells; left panel. Heatmap of Th2_DC genes expression on skin myeloid cells; right upper panel. Heatmap of Th2_DC genes expression on PBMC myeloid cells; right lower panel. (C) Correlation of all sample's migDC1 proportions to Th2-cell proportions. (D) Heatmap of cytotoxic gene expression in NK cells by each sample. (E) AD6 lesional skin and Th2_DC, Th2 scoring; upper panel. Annotation of AD6 non-lesional skin and Th2_DC, Th2 scoring; lower panel (DE junction; dermis epidermis junction, LEC; lymphatic endothelial cell). Each score of genes is listed below. (F) Percentage of pSTAT6-positive cDC in total cDC (G) Notch2 expression histogram of 5 nM rhIL-13 stimulated total cDC in pSTAT6(−/+); upper panel. CD206 histogram of rhIL-13 5 nM stimulated cDC in pSTAT6(−/+); lower panel. The plots are representative from PBMCs of 12 AD donor, 12 HC donor (rhIL-13; recombinant human interleukin-13).

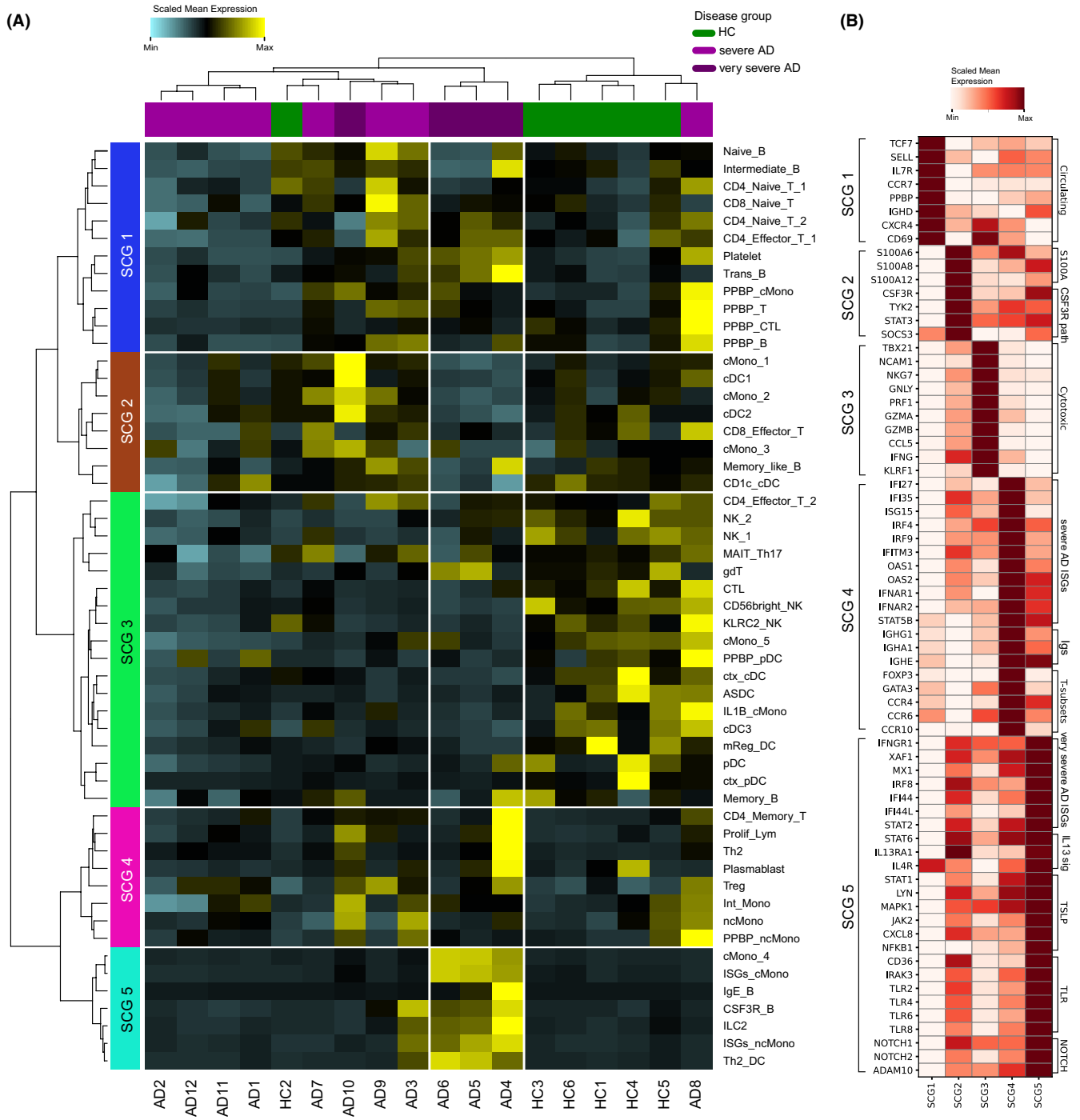

FIGURE 6 Patient stratification via proportions displayed characteristic of each disease group. (A) Heatmap showing proportions of each cell type cluster. Hierarchical clustering for individual subjects and cell types resulted in five subcluster groups of cell types. (B) Characteristic genes for each subcluster group compared to the other subcluster groups. Genes were categorized by functional similarity.

to other DC2 subsets, DC^{Th2} express lower levels of interferon response genes.[18] Consistent with this, Th2_DC in our dataset demonstrated elevation of the IL-13 receptor complex (*IL13RA1* and *IL4R*) and its downstream signal partner *STAT6* (Figure S4C,D). Moreover, Th2_DC expressed minimal interferon responses while exhibiting high levels of *TLR4*. Significant expression of various transcription factors (*IRF4*, *FOXO4*, *NFKB1*, *NFATC1*, and *STAT5B*) in Th2_DC (Figure 4D,G,H) suggests that their possible circulation into peripheral blood governed by skin-homing factors (integrin alpha4 beta1 complex and *CCR2*) (Figure 4D). Although potential activating interactions such as *ICAM3-LFA1*, *CD47-SIRPG*, and *TNFSF13-TNFRSF14* were identified, the DC signals that drive the development of the Th2 response require further investigation. Interestingly, Notch signaling was predominant in Th2_DC among all DC subsets (Figure S4A,C). Given that Notch signaling affects myeloid cell differentiation, including that of DCs,[51] it may play

a role in Th2_DCs differentiation. Additionally, the MigDC_1 subset in skin shows mature DC and Th2_DC signals simultaneously (Figure 5B and Figure S6B). MigDC_1, akin to Th2_DC, represents a Type 2 response enriched with IL13 signals and is expanded in AD (Figure S6C). Using the same Th2_DC gene set, Th2_DC was found in the upper dermis of spatially lesional AD skin, where immune cells also strongly exhibited Th2 cell scores (Figure 5E). Experimental validation involved stimulating DCs with rhIL-13, confirming the presence of IL13RA1 downstream signaling (pSTAT6), along with CD206 (MRC1) and Notch2 in IL-13-responsive DCs (pSTAT6(+)) compared to the nonresponsive DCs (pSTAT6(−)). This validation, by using the same patient samples used in the scRNA-Seq analysis and an additional cohort, reinforced our observation (Figure 5F,G and Figure S7B,C). Thus, our findings suggest an expansion of AD-associated DCs, marked by Notch2 and CD206, responsive to Type II immune signals, potentially playing a role in priming Th2 cells.

Although JAK inhibitors have been in the spotlight for the treatment of AD, *JAK1* was not a characteristic feature of AD in our subgroup analysis, unlike *JAK2* (Figure 6). We hypothesized that elevated *JAK1* and *STAT4* expression in cytotoxic cells (SCG3, Figure S8C), which is reduced in AD alongside decreased cytotoxicity. However, in monocytes and DCs, the innate immune myeloid cell populations that undergo alterations in AD patients (Figures 3 and 4), *JAK1* exhibited increased expression in almost all myeloid subpopulations in AD patients compared to HCs (Figure S8D). Notably, *JAK1* expression was not elevated in the lymphoid cells of AD (T, NK, and ILCs). On the other hand, *JAK2*, *JAK3*, and *TYK2* were upregulated in both lymphoid and myeloid cells in AD.

In conclusion, our study underscores the importance of understanding AD as a systemic immune disorder with notable alterations in Th2 cells, NK cell function, and specific monocyte subsets. The identification of AD-associated Th2_DC cells suggests a crucial role in the Th2 immune response. These findings reshape the understanding of AD pathology, offering insights for future research and precision therapeutic strategies.

AUTHOR CONTRIBUTIONS

Analysis and writing: SJ, KL, and SH. Conceptualization: DHL and HJK. Data generation and acquisition: YJB, SJ, SC, JSL, CP, HJK, and JK. Computational analysis and data interpretation: KL. Flow cytometry: YHJ. Supervision: EGY, HJK, SH, and DHL. Writing: SJ, KL, SH, and DHL.

ACKNOWLEDGEMENTS

None.

FUNDING INFORMATION

Bio & Medical Technology Development Program of the National Research Foundation (NRF) was funded by the Ministry of Science & ICT 2022M3A9D3016848 (DHL and HJK), the Ministry of Education 2020R1F1A1073692 (HJK), 2022R1F1A1075235 (SPJ), and 2022R1A2C10066566 (SH) and the Yonsei University Research Fund of 2022-22-0296 (SH).

CONFLICT OF INTEREST STATEMENT

The authors declare no competing financial interest.

DATA AVAILABILITY STATEMENT

Data of this study are available from the corresponding author upon reasonable request.

ORCID

Seon-Pil Jin https://orcid.org/0000-0002-8290-4278
Kyungchun Lee https://orcid.org/0009-0001-5075-2767
Hyun Je Kim https://orcid.org/0000-0002-4184-6702
Seunghee Hong https://orcid.org/0000-0002-0134-1195
Dong Hun Lee https://orcid.org/0000-0002-2925-3074

REFERENCES

1. Laughter MR, Maymone MBC, Mashayekhi S, et al. The global burden of atopic dermatitis: lessons from the global burden of disease study 1990–2017. *Br J Dermatol*. 2021;184(2):304-309.
2. Czarnowicki T, He H, Krueger JG, Guttman-Yassky E. Atopic dermatitis endotypes and implications for targeted therapeutics. *J Allergy Clin Immunol*. 2019;143(1):1-11.
3. Suarez-Farinas M, Dhingra N, Gittler J, et al. Intrinsic atopic dermatitis shows similar TH2 and higher TH17 immune activation compared with extrinsic atopic dermatitis. *J Allergy Clin Immunol*. 2013;132(2):361-370.
4. Noda S, Suarez-Farinas M, Ungar B, et al. The Asian atopic dermatitis phenotype combines features of atopic dermatitis and psoriasis with increased TH17 polarization. *J Allergy Clin Immunol*. 2015;136(5):1254-1264.
5. He H, Suryawanshi H, Morozov P, et al. Single-cell transcriptome analysis of human skin identifies novel fibroblast subpopulation and enrichment of immune subsets in atopic dermatitis. *J Allergy Clin Immunol*. 2020;145(6):1615-1628.
6. Mashiko S, Mehta H, Bissonnette R, Sarfati M. Increased frequencies of basophils, type 2 innate lymphoid cells and Th2 cells in skin of patients with atopic dermatitis but not psoriasis. *J Dermatol Sci*. 2017;88(2):167-174.
7. Honda T, Kabashima K. Reconciling innate and acquired immunity in atopic dermatitis. *J Allergy Clin Immunol*. 2020;145(4):1136-1137.
8. Bangert C, Rindler K, Krausgruber T, et al. Persistence of mature dendritic cells, T(H)2A, and Tc2 cells characterize clinically resolved atopic dermatitis under IL-4Ralpha blockade. *Sci Immunol*. 2021;6(55):eabe2749.
9. Pavel AB, Zhou L, Diaz A, et al. The proteomic skin profile of moderate-to-severe atopic dermatitis patients shows an inflammatory signature. *J Am Acad Dermatol*. 2020;82(3):690-699.
10. Liu Y, Wang H, Taylor M, et al. Classification of human chronic inflammatory skin disease based on single-cell immune profiling. *Sci Immunol*. 2022;7(70):eabl9165.
11. Renert-Yuval Y, Del Duca E, Pavel AB, et al. The molecular features of normal and atopic dermatitis skin in infants, children, adolescents, and adults. *J Allergy Clin Immunol*. 2021;148(1):148-163.
12. Kumar N, Mishra B, Athar M, Mukhtar S. Inference of gene regulatory network from single-cell transcriptomic data using pySCENIC. *Methods Mol Biol*. 2021;2328:171-182.
13. He Y, Luo J, Zhang G, et al. Single-cell profiling of human CD127(+) innate lymphoid cells reveals diverse immune phenotypes in hepatocellular carcinoma. *Hepatology*. 2022;76(4):1013-1029.
14. Alkon N, Bauer WM, Krausgruber T, et al. Single-cell analysis reveals innate lymphoid cell lineage infidelity in atopic dermatitis. *J Allergy Clin Immunol*. 2022;149(2):624-639.

15. Lessel D, Gehbauer C, Bramswig NC, et al. BCL11B mutations in patients affected by a neurodevelopmental disorder with reduced type 2 innate lymphoid cells. *Brain*. 2018;141(8):2299-2311.
16. Mjosberg J, Spits H. Human innate lymphoid cells. *J Allergy Clin Immunol*. 2016;138(5):1265-1276.
17. Lewis KL, Caton ML, Bogunovic M, et al. Notch2 receptor signaling controls functional differentiation of dendritic cells in the spleen and intestine. *Immunity*. 2011;35(5):780-791.
18. Mayer JU, Hilligan KL, Chandler JS, et al. Homeostatic IL-13 in healthy skin directs dendritic cell differentiation to promote TH2 and inhibit TH17 cell polarization. *Nat Immunol*. 2021;22(12):1538-1550.
19. Williams JW, Tjota MY, Clay BS, et al. Transcription factor IRF4 drives dendritic cells to promote Th2 differentiation. *Nat Commun*. 2013;4:2990.
20. Chuvpilo S, Avots A, Berberich-Siebelt F, et al. Multiple NF-ATc isoforms with individual transcriptional properties are synthesized in T lymphocytes. *J Immunol*. 1999;162(12):7294-7301.
21. Tang W, Lu Y, Tian QY, et al. The growth factor progranulin binds to TNF receptors and is therapeutic against inflammatory arthritis in mice. *Science*. 2011;332(6028):478-484.
22. Zhao H, Yan M, Wang H, Erickson S, Grewal IS, Dixit VM. Impaired c-Jun amino terminal kinase activity and T cell differentiation in death receptor 6-deficient mice. *J Exp Med*. 2001;194(10):1441-1448.
23. Seiffert M, Brossart P, Cant C, et al. Signal-regulatory protein alpha (SIRPalpha) but not SIRPbeta is involved in T-cell activation, binds to CD47 with high affinity, and is expressed on immature CD34(+) CD38(−) hematopoietic cells. *Blood*. 2001;97(9):2741-2749.
24. Jiang P, Lagenaur CF, Narayanan V. Integrin-associated protein is a ligand for the P84 neural adhesion molecule. *J Biol Chem*. 1999;274(2):559-562.
25. Shurin MR, Ma Y, Keskinov AA, et al. BAFF and APRIL from Activin A-treated dendritic cells upregulate the antitumor efficacy of dendritic cells in vivo. *Cancer Res*. 2016;76(17):4959-4969.
26. Piccio L, Vermi W, Boles KS, et al. Adhesion of human T cells to antigen-presenting cells through SIRPbeta2-CD47 interaction costimulates T-cell proliferation. *Blood*. 2005;105(6):2421-2427.
27. Andre P, Spertini O, Guia S, et al. Modification of P-selectin glycoprotein ligand-1 with a natural killer cell-restricted sulfated lactosamine creates an alternate ligand for L-selectin. *Proc Natl Acad Sci USA*. 2000;97(7):3400-3405.
28. Visser L, de Vos AF, Hamann J, et al. Expression of the EGF-TM7 receptor CD97 and its ligand CD55 (DAF) in multiple sclerosis. *J Neuroimmunol*. 2002;132(1–2):156-163.
29. Leemans JC, te Velde AA, Florquin S, et al. The epidermal growth factor-seven transmembrane (EGF-TM7) receptor CD97 is required for neutrophil migration and host defense. *J Immunol*. 2004;172(2):1125-1131.
30. Legler DF, Krause P, Scandella E, Singer E, Groettrup M. Prostaglandin E2 is generally required for human dendritic cell migration and exerts its effect via EP2 and EP4 receptors. *J Immunol*. 2006;176(2):966-973.
31. DeTomaso D, Jones MG, Subramaniam M, Ashuach T, Ye CJ, Yosef N. Functional interpretation of single cell similarity maps. *Nat Commun*. 2019;10(1):4376.
32. Mitamura Y, Reiger M, Kim J, et al. Spatial transcriptomics combined with single-cell RNA-sequencing unravels the complex inflammatory cell network in atopic dermatitis. *Allergy*. 2023;78(8):2215-2231.
33. Meenhuis A, Irandoust M, Wolfler A, Roovers O, Valkhof M, Touw IP. Janus kinases promote cell-surface expression and provoke autonomous signalling from routing-defective G-CSF receptors. *Biochem J*. 2009;417(3):737-746.
34. Thyssen JP, Vestergaard C, Deleuran M, et al. European task force on atopic dermatitis (ETFAD): treatment targets and treatable traits in atopic dermatitis. *J Eur Acad Dermatol Venereol*. 2020;34(12):e839-e842.
35. Bieber T. Atopic dermatitis: an expanding therapeutic pipeline for a complex disease. *Nat Rev Drug Discov*. 2022;21(1):21-40.
36. He H, Del Duca E, Diaz A, et al. Mild atopic dermatitis lacks systemic inflammation and shows reduced nonlesional skin abnormalities. *J Allergy Clin Immunol*. 2021;147(4):1369-1380.
37. Katsuta M, Takigawa Y, Kimishima M, Inaoka M, Takahashi R, Shiohara T. NK cells and gamma delta+ T cells are phenotypically and functionally defective due to preferential apoptosis in patients with atopic dermatitis. *J Immunol*. 2006;176(12):7736-7744.
38. Mack MR, Brestoff JR, Berrien-Elliott MM, et al. Blood natural killer cell deficiency reveals an immunotherapy strategy for atopic dermatitis. *Sci Transl Med*. 2020;12(532):eaay1005.
39. Mobus L, Rodriguez E, Harder I, et al. Blood transcriptome profiling identifies 2 candidate endotypes of atopic dermatitis. *J Allergy Clin Immunol*. 2022;150(2):385-395.
40. Freud AG, Keller KA, Scoville SD, et al. NKp80 defines a critical step during human natural killer cell development. *Cell Rep*. 2016;16(2):379-391.
41. Simpson EL, Parnes JR, She D, et al. Tezepelumab, an anti-thymic stromal lymphopoietin monoclonal antibody, in the treatment of moderate to severe atopic dermatitis: a randomized phase 2a clinical trial. *J Am Acad Dermatol*. 2019;80(4):1013-1021.
42. Laquer V, Parra V, Lacour JP, et al. Interleukin-33 antibody failed to demonstrate benefit in a phase II, double-blind, randomized, placebo-controlled study in adult patients with moderate-to-severe atopic dermatitis. *Br J Dermatol*. 2022;187(4):599-602.
43. Sarrias MJ, Artigas F, Martinez E, et al. Decreased plasma serotonin in melancholic patients: a study with clomipramine. *Biol Psychiatry*. 1987;22(12):1429-1438.
44. Lamiable O, Mayer JU, Munoz-Erazo L, Ronchese F. Dendritic cells in Th2 immune responses and allergic sensitization. *Immunol Cell Biol*. 2020;98(10):807-818.
45. Kumamoto Y, Linehan M, Weinstein JS, Laidlaw BJ, Craft JE, Iwasaki A. CD301b(+) dermal dendritic cells drive T helper 2 cell-mediated immunity. *Immunity*. 2013;39(4):733-743.
46. Gao Y, Nish SA, Jiang R, et al. Control of T helper 2 responses by transcription factor IRF4-dependent dendritic cells. *Immunity*. 2013;39(4):722-732.
47. Klein U, Casola S, Cattoretti G, et al. Transcription factor IRF4 controls plasma cell differentiation and class-switch recombination. *Nat Immunol*. 2006;7(7):773-782.
48. Eguchi J, Kong X, Tenta M, Wang X, Kang S, Rosen ED. Interferon regulatory factor 4 regulates obesity-induced inflammation through regulation of adipose tissue macrophage polarization. *Diabetes*. 2013;62(10):3394-3403.
49. Bell BD, Kitajima M, Larson RP, et al. The transcription factor STAT5 is critical in dendritic cells for the development of TH2 but not TH1 responses. *Nat Immunol*. 2013;14(4):364-371.
50. Ito T, Wang YH, Duramad O, et al. TSLP-activated dendritic cells induce an inflammatory T helper type 2 cell response through OX40 ligand. *J Exp Med*. 2005;202(9):1213-1223.
51. Cheng P, Gabrilovich D. Notch signaling in differentiation and function of dendritic cells. *Immunol Res*. 2008;41(1):1-14.

SUPPORTING INFORMATION

Additional supporting information can be found online in the Supporting Information section at the end of this article.

How to cite this article: Jin S-P, Lee K, Bang YJ, et al. Mapping the immune cell landscape of severe atopic dermatitis by single-cell RNA-seq. *Allergy*. 2024;79:1584-1597. doi:10.1111/all.16121